WAVEFRONT SENSING TECHNOLOGY FOR ADAPTIVE OPTICAL SYSTEMS

Tae-Kyoung Uhm[a], Kyung-Wan Roh[b], Ji-Yeon Kim[b], Kang-Soo Park[b], Jun-Ho Lee[c] and Sung-Kie Youn[b]

[a,b]Department of Mechanical Engineering
Korea Advanced Institute of Science and Technology

[c]Department of Applied Optics
Kongju National University

[a]espoir@kaist.ac.kr

ABSTRACT:

Remote sensing through atmospheric turbulence had been hard works for a long time, because wavefront distortion due to the Earth's atmospheric turbulence deteriorates image quality. But due to the appearance of adaptive optics, it is no longer difficult things. Adaptive optics is the technology to correct random optical wavefront distortions in real time. For past three decades, research on adaptive optics has been performed actively. Currently, most of newly built telescopes have adaptive optical systems.

Adaptive optical system is typically composed of three parts, wavefront sensing, wavefront correction and control. In this work, the wavefront sensing technology for adaptive optical system is treated. More specifically, shearing interferometers and Shack-Hartmann wavefront sensors are considered. Both of them are zonal wavefront sensors and measure the slope of a wavefront.

In this study, the shearing interferometer is made up of four right-angle prisms, whose relative sliding motions provide the lateral shearing and phase shifts necessary for wavefront measurement. Further, a special phase-measuring least-squares algorithm is adopted to compensate for the phase-shifting error caused by the variation in the thickness of the index-matching oil between the prisms.

Shack-Hartmann wavefront sensors are widely used in adaptive optics for wavefront sensing. It uses an array of identical positive lenslets. And each lenslet acts as a subaperture and produces spot image. Distortion of an input wavefront changes the location of spot image. And the slope of a wavefront is obtained by measuring this relative deviation of spot image.

Structures and measuring algorithms of each sensor will be presented. Also, the results of wavefront measurement will be given. Using these wavefront sensing technology, an adaptive optical system will be built in the future.

KEY WORDS: Adaptive Optics, Shearing Interferometer, Shack-Hartmann Sensor, Wavefront Sensing

1. INTRODUCTION TO ADAPTIVE OPTICS

1.1 Adaptive Optics

Peering into the night skies, one can find twinkling stars. These may sound romantic, but twinkling of stars had given difficulties to astronomers observing the stars for a long time. Twinkling of stars is caused by the Earth's atmospheric turbulence. Small local variation in atmospheric temperature causes random changes in wind velocity and the atmospheric density. And the changes in the atmospheric density give rise to small local changes in the index of refraction. In this point of view, the atmosphere can be regarded as 'the collection of small lenses' of which characteristics change in real time. By this atmospheric turbulence, the wavefront of a beam is distorted. And the image through the atmosphere is blurred.

Adaptive optics can be a good solution. Adaptive optics is the technology for correcting random optical wavefront distortions in real time. It started with the desire to control and improve image formation in earth-based telescope. Its history is short. But, research on adaptive optics has been performed actively and currently, most of newly built telescopes adopt adaptive optical systems. Adaptive optics is composed of three subsystems. [Figure 1.] (Hardy, 1998; Tyson, 1997) A wavefront sensor measures the distortion induced by the atmosphere by evaluating the light from a natural source or an artificial beacon placed high above the telescope. An active mirror, called a deformable mirror, can rapidly change its surface shape to match the phase distortions measured by the wavefront sensor. A control computer is used to evaluate the wavefront sensor measurements and translate the signals into control signals to drive the actuators of the deformable mirror.

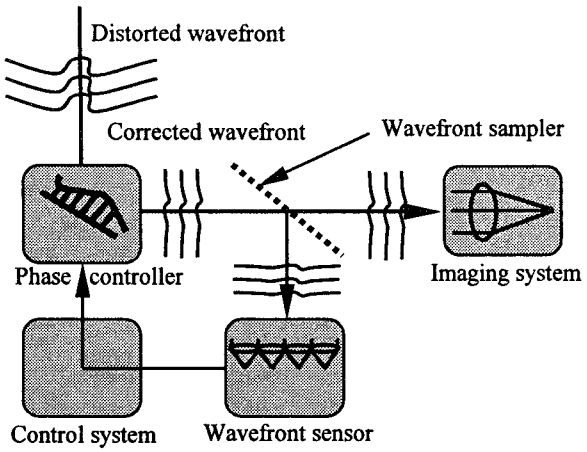

Figure 1. A schematic diagram of a conventional adaptive optical system.

1.2 Wavefront Sensing Technology in Adaptive Optics

The wavefront sensing techniques used in adaptive optics fall into following two main classes, i.e. zonal and modal wavefront sensing.

I. Zonal wavefront sensing
  1. Wavefront slope sensing
    a. Shack-Hartmann sensor
    b. Lateral shear interferometer
  2. Wavefront curvature sensing
    a. Curvature sensor
II. Modal wavefront sensing
  1. Overall tilt sensing
  2. Focus sensing

In this paper, as the wavefront sensing technology for adaptive optical system, shearing interferometers and Shack-Hartmann wavefront sensors are considered. Both of them are zonal wavefront sensors and measure the slope of a wavefront.

2. SHEARING INTERFEROMETER

2.1 Interferometer Design

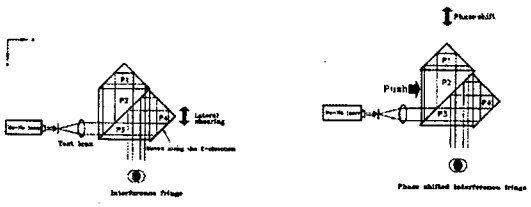

(a) (b)

Figure 2. (a) Lateral shearing and (b) phase shifting mechanism

The shearing interferometer configured in this paper is shown in Figure 2 and 3. The lens under inspection is tested by examining the wavefront of the beam that is generated by the lens. For that, a parallel beam is made by the lens. The collimated beam would be a plane wave if the lens is perfectly free of aberrations. Otherwise, it would have a distorted wavefront. The interferometer is composed of four pieces of prisms. For convenience, the prisms are designated P1, P2, P3 and P4, respectively. They are directly attached to each other using index-matching oil so that relative sliding motions between the prisms are allowed.

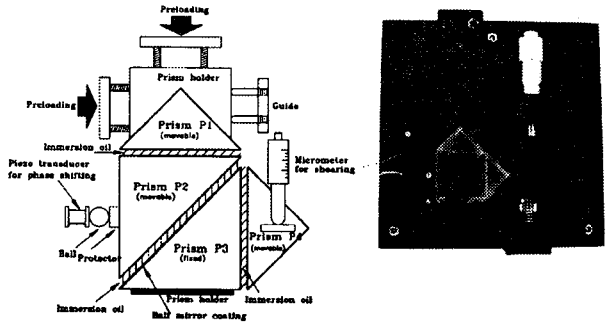

Figure 3. Mechanical design and photograph of the shearing interferometer

Lateral shearing is provided by sliding prism P4 in the z direction, as illustrated in Figure 2(a). In addition, phase shifts are introduced by pushing prism P2 along the inclined surface of prism P3 as illustrated in Figure 2(b). The prism P1 is constrained to move only in the z direction. Thus the movement of prism P2 in the x and z directions causes no lateral shearing in the x direction, but only changes the optical path in the z direction, inducing phase shifting. Figure 3 shows in detail how the optical components of the interferometer are secured mechanically. Prism P4 is adjusted by a micrometer to set a predetermined amount of lateral shearing prior to measurement. A piezoelectric actuator is used to push prism P2 in steps during measurement to generate a series of phase shifts. Prism P1 is kinematically guided by a set of preloaded springs to move only in the x direction.

2.2 Phase Measurement

In this type of lateral shearing interferometer, one problem is that the amounts of phase shifts are not easy to precisely control, because the index-matching oil is squeezed out when the prisms are moved for phase shifting. Thus, the oil thickness does not remain constant, causing a significant level of inaccuracy in phase shifting. This problem with phase shift errors can be effectively overcome by using the least-squares phase-measuring algorithm. (Han, 1994; Kong, 1995) In this algorithm, true values of phase shifts can be identified directly from interferograms. This algorithm uses a least-squares technique in which a residual error function related to phase shift errors is minimized to determine true solutions of phase shifts.

The first step of the least-squares phase-measuring algorithm is to define the differential intensity such as

$$J_{ij} = I_{ij} - I_{i0} = C_i(\cos\delta_j - 1) + S_i \sin\delta_j \quad (1)$$

In fact, the differential intensity J_{ij} represents the variation of intensity induced by the phase shift δ_j, assuming $\delta_0 = 0$. Then, besides C_i and S_i, δ_j are also treated as unknowns and they are to be determined so as to minimize the residual function of

$$E = (J_{ij} - J_{ij}^*)^2 = \left[C_i(\cos\delta_j - 1) + S_i \sin\delta_j - J_{ij}^*\right]^2 \quad (2)$$

where J_{ij}^* denotes the measured value of J_{ij}. The necessary conditions for the minimization of the function E is given by

$$\partial E/\partial C_i = \partial E/\partial S_i = \partial E/\partial \delta_j = 0 \quad (3)$$

These equations can be readily solved. When δ_j, C_i and S_i are obtained, the slope of a wavefront $\Delta w(x,y)$ is subsequently determined by

$$\Delta w(x,y) = \phi_i / k = (1/k)\tan^{-1}(S_i / C_i) \quad (4)$$

Finally, the wavefront $w(x,y)$ is computed by the integration of Eq. (4). Once the wavefront $w(x,y)$ is determined, the aberrations of the lens are analyzed by fitting the Zernike polynomials in which the Gram-Schmidt orthogonalization method is usefully adopted.

2.3 Experimental Results

A typical shearing interferogram obtained from the interferometer built in this study is shown in Figure 4. Here, a collimating lens is used as the test lens.

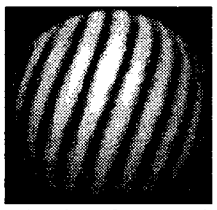

Figure 4. Typical shearing interferogram by the lateral-shearing interferometer

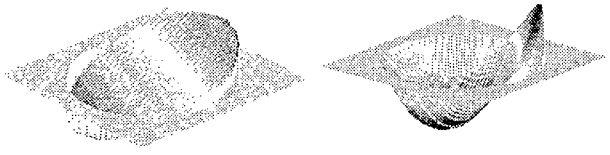

(a) (b)

Figure 5. (a) Slope of a wavefront and (b) the wavefront shape

To compute the slope of a wavefront, a series of interferograms are generated by inducing phase shifts sequentially four times. The least-squares phase-measuring algorithm is then used to suppress the phase shift errors caused by the thickness variation of the index-matching oil. The slope of a wavefront is determined as shown in Figure 5(a). Finally, the wavefront is constructed by integrating the slope of a wavefront as presented in Figure 5(b). From this result, the rms wavefront error is 0.7λ at λ=632.8nm.

3. SHACK-HARTMANN SENSOR

3.1 Shack-Hartmann Sensor Design

The Shack-Hartmann sensor configured in this paper is shown in Figure 6. It is composed of two main components, a lenslet array of OKO Tech. and a digital CMOS camera of Basler. The lenslet array is 16×16 orthogonal type. Its picth is 0.3mm and the focusing length is 40mm. The pixel resolution of CMOS camera is 659×491 and the maximum frame rate is 100fps. In this design, relay optics is not used because the beam diameter through the lenslet array and the area of the CMOS sensor are approximately same. As shown in Figure 6, the beam from a laser source is collimated by a collimating lens. And the diameter and intensity of the beam are adjusted by an iris diaphragm and a ND filter, respectively. Then, the beam is focused to the CMOS camera by the lenslet array. From this path, spot images are obtained. If there are no aberrations, the array of spots should be exactly orthogonal. But if there are aberrations, the positions of spots are changed from the original ones. The slope of a wavefront is obtained by measuring the deviation of spots.

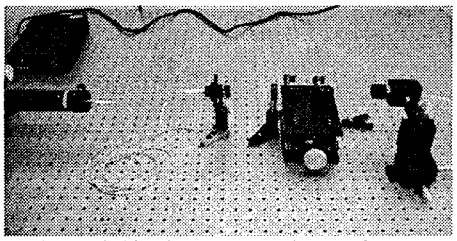

Figure 6. Shack-Hartmann Sensor System

3.2 Wavefront Measurement Algorithm

The wavefront measurement algorithm of Shack-Hartmann sensors is mainly composed of three parts, searches for spot centroids, slope calculation and wavefront reconstruction. The detailed flow of the algorithm is followed. Firstly, the centroid of each spot is searched for the reference and test spot images. Then, the deviation of spots in relation to the reference spot positions can be obtained. The centroids of spots can be simply calculated by center of mass algorithm, Eq. (5). Generally, this algorithm is used with other noise reduction algorithm such as thresholding and windowing etc. In this study, thresholding is used to reduce noise.

$$C_x = \frac{\sum_{i=0}^{N}\sum_{j=0}^{N} I_{i,j} \times x_i}{\sum_{i=0}^{N}\sum_{j=0}^{N} I_{i,j}} \quad C_y = \frac{\sum_{i=0}^{N}\sum_{j=0}^{N} I_{i,j} \times y_i}{\sum_{i=0}^{N}\sum_{j=0}^{N} I_{i,j}} \tag{5}$$

where $I_{i,j}$ =optical intensity at (i, j) th pixel

$N \times N$ = the number of pixels in a subaperture

Once the deviation is obtained, the slope of a wavefront can be calculated directly by Eq. (6).

$$S_x = \frac{(C_x - C_{x,ref}) \cdot d_x}{F} \quad S_y = \frac{(C_y - C_{y,ref}) \cdot d_y}{F} \tag{6}$$

where F = the focusing length of a lenslet array

$(C_{x,ref}, C_{y,ref})$ = the coordinate of the centroid in the reference spot

d_x, d_y = the length of one pixel in a CCD along the x and y axes

In the next step, the wavefront are reconstructed using the obtained slope of a wavefront. There are some kinds of wavefront reconstruction algorithms. As zonal methods, there exists Southwell, Fried and Hudgin models according to geometry of gradient vectors and wavefront points. In this study, the Southwell reconstruction model is used. The comparison of zonal reconstruction algorithms through pre-simulations shows that the Southwell model has more exact reconstructing performance. Figure 7 shows the Southwell wavefront reconstruction model and by Eq. (7), the wavefront is determined.

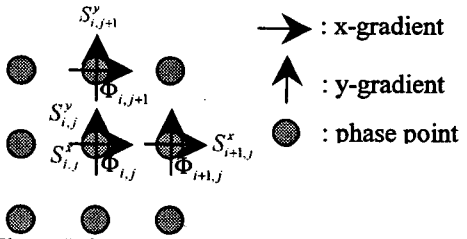

Figure 7. Southwell wavefront reconstruction model

$$\frac{S^x_{i+1,j} + S^x_{i,j}}{2} = \frac{(\Phi_{i+1,j} - \Phi_{i,j})}{h} \tag{7}$$
$$\frac{S^y_{i,j+1} + S^y_{i,j}}{2} = \frac{(\Phi_{i,j+1} - \Phi_{i,j})}{h}$$

where $\Phi_{i,j}$ = wavefront at the (i, j) th phase point

h = the distance between adjacent phase points

Once the wavefront is determined, the aberrations can be analyzed by fitting the Zernike polynomials

3.3 Experimental Results

Figure 8 shows a typical spot image by the Shack-Hartmann sensor. For wavefront measurement, a reference spot image is firstly taken. Then, random wavefront distortion is made. And again, spot images are taken. Sequentially taken spot images are processed as stated before. Figure 9 shows the final results. In this results, the rms wavefront error is 0.073λ at λ=632.8nm.

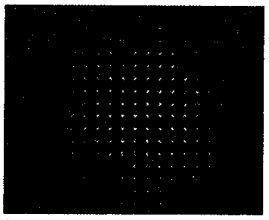

Figure 8. Typical spot image by the Shack-Hartmann sensor

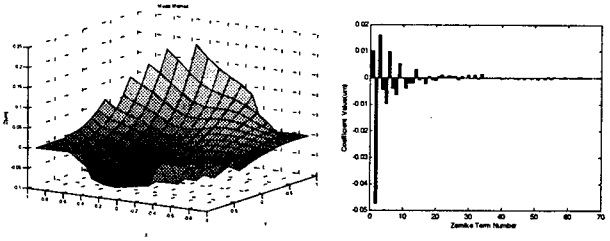

(a) (b)

Figure 9. (a) the wavefront shape and (b) Zernike coefficients

4. CONCLUSION

In this study, wavefront sensing technology for adaptive optical systems was treated. Especially, a lateral shearing interferometer and a Shack-Hartmann sensor was built and the wavefront measurement was performed by using them. Currently, they don't work in real time. But in the future, they are supposed to work in real time and have improved performance. And finally, the whole adaptive optical system will be constructed.

References from Journals:

G.-S. Han and S.-W. Kim, 1994. Numerical correction of reference phases in phase-shifting interferometry by iterative least-squares fitting. *Appl. Opt.*, 33, pp. 7321-7325.

I.-B. Kong and S.-W. Kim, 1995. General algorithm of phase-shifting interferometry by iterative least-squares fitting. *Opt. Eng.*, 34, pp. 183-188.

References from Books:

John W. Hardy, 1998. *Adaptive Optics for Astronomical Telescopes*. Oxford University Press, New York, pp. 135-307.

Robert K. Tyson, 1997. *Principles of Adaptive Optics*. Academic Press, San Diego, pp. 121-275.

Acknowledgements

This research was supported by the Agency for Defense Development, Korea, through the Image Information Research Center at Korea Advanced Institute of Science & Technology.